(Received 25 December 2025, Accepted 30 January 2026, Scheduled 18 April 2026)

Two-Tone IMD3 and IMD5 Models of Weakly Nonlinear GaN Amplifier for Tx-Rx Microwave and Millimeter-Wave Systems

Jiahao Li[1], Fayu Wan[1], Junkun Wan[2], Nathan B. Gurgel[3], Sébastien Lallechere[4], Nicolas Waldhoff[5], Dmitry Kholodnyak[6], Glauco Fontgalland[7], and Blaise Ravelo[1, *]

[1] *Nanjing University of Information Science & Technology (NUIST), Nanjing 210044, Jiangsu, China*
[2] *Chien-Shiung Wu College, Southeast University, Nanjing, China*
[3] *Applied Electromagnetic and Microwave Laboratory, Federal University of Campina Grande, Campina Grande 58429, Brazil*
[4] *Association Française de Science des Systémes (AFSCET), 3 ter rue d'Estienne d'Orves, Fontenay-aux-Roses 92260, France*
[5] *Unite de Dynamique de Structure des Matériaux Moléculaires (UDSMM) Université de Littoral Côte d'Opale (ULCO), 145, Avenue Maurice Schumann, Dunkerque 59140, France*
[6] *Department of Microwave Electronics, Saint Petersburg Electrotechnical University "LETI", Saint Petersburg, Russia*
[7] *Brenton School of Engineering, University of Mount Union, Alliance, OH 44601, USA*

ABSTRACT: With the increase in users' demand, the wireless communication systems are expected to operate by considering microwave and millimeter wave signals under higher power intensity by means of multichannel propagation. Therefore, the nonlinear (NL) effect becomes a major challenge to maintain the communication system performance. To deal with such an undesirable effect, the microwave amplifier (MA) NL characterization requires a relevant modelling technique. The intermodulation distortion (IMD) constitutes one of the basic approaches for MA NL analyses. The IMD of the MA two-tone (TT) response in weakly NL behavior is modelled and measured in this paper. The modelling method is empirically derived from the Volterra series coefficients of the MA input-output characteristic from a single-tone (ST) test. The m^{th}-order IM amplitudes of MA NL TT response are formulated as a function of the ST odd harmonics. The efficiency of the IM(m) models is experimentally validated with TT measurements of Gallium Nitride MAs around 2.4 GHz and 24 GHz carrier frequencies. The behavior of the IMD3 and IMD5 of weakly NL (WNL) models around 2.4 GHz is in good agreement with the TT input amplitude measured from -25 to -5 dBm. The IMD3 WNL model around 24 GHz is also well-correlated to measurement with input amplitude range from -20 to -3 dBm. In the future, the developed NL model can be exploited for assessing the MA impact on the microwave system communication performance.

1. INTRODUCTION

To meet the constant increase of users' demand, the 5G and 6G wireless communication systems are expected to integrate complex electronic functions and to operate with higher speed data. Thanks to the increase of integration density and operation frequency channel saturation, the electromagnetic interference (EMI) is among the open research problems listed by the visioners to limit the performance of future wireless systems [1].

Relevant technical solutions dedicated to the EMI analyses and characterizations must be developed with respect to the design and fabrication technology progress in order to minimize imperfections of the communication systems.

Therefore, nowadays, analysis of EMI effect in radio frequency (RF) and microwave amplifiers (MAs) becomes a hot topic of design, fabrication, and test researchers for the communication system characterization [2–4]. Different EMI analysis approaches forwarding prediction [3] and analysis techniques to study MA nonlinear (NL) effects for wireless transceivers [4] were proposed in the literature. A competitive study about the NL characterization is an open challenge for all RF/microwave and millimeter (mm) wave design, fabrication, and test research engineers.

In fact, the EMI and MA NL studies have usually been developed by means of the intermodulation (IM) analysis [5–10]. The NL analysis building block consists in the input-output power characterization by means of the two-tone (TT) testing [5–8]. The TT test has been recently exploited for the EMI characterization of Gallium Nitride (GaN) MAs [7, 8]. As the NL test is time costly and does not enable fundamental understanding of the MA behavior, a relevant modelling is necessary [9, 11].

The IM distortion (IMD) caused by active microwave component NL effects constitutes one of the main parameters to be assessed to predict the communication system performance. There are several approaches to assessing the IMDs related to the communication signal distortions. Traditionally, the IMDs can be analyzed by using the Volterra series representation [12, 13], state-space approach [14], symbolic model [15], and efficient parameter sensitivity computation [16]. The phenomena of EMI-induced distortion were modelled with NL effect for feedback MA [17]. However, the IM modelling with consideration of harmonics of higher than third-order remains a challenging task.

* Corresponding author: Blaise Ravelo (blaise.ravelo@yahoo.fr).

For this reason, the present paper develops the IM analytical models by means of the MA TT response. The modelling principle consists in formulating the IM as a function of the Volterra series NL coefficients, which are determined from the single-tone (ST) test. As challenging active components are used as solutions for current microwave and mm-wave systems, and two different GaN MAs are designed and prototyped as devices under tests (DUTs). The experimental investigation of this work was carried out at microwave and mm-wave frequencies, $f_{01} = 2.4\,\text{GHz}$ and $f_{02} = 24\,\text{GHz}$, which are investigated, respectively.

The core innovation of the present work is to develop a practical methodology that bridges two different techniques dedicated to the MA characterization. The proposed modelling method extracts, from empirical rapid ST measurements, the Volterra series-based nonlinear coefficients of the polynomial relationship between input and output voltages. Then, these coefficients will be utilized to predict analytically IMD3 and IMD5 of the MA TT test. The method provides a faster pathway for device characterization compared to starting directly with complex TT tests. The effectiveness of this ST-to-TT prediction is not merely a theoretical approach. For this reason, it is rigorously validated through measurements on two distinct GaN amplifiers at f_{01} (microwave) and f_{02} (millimeter-wave), demonstrating its applicability across frequency bands relevant to modern communications.

To do this, the paper is organized into seven sections:

- Section 2 focuses on the general theory of the modelling of high-order (more than 2nd order) IMs corresponding to the different NL zone effects undesirably generated by a MA.
- Section 3 describes the experimental setup based on the ST and TT automatic testing for the MA NL characterization, enabling the measurement of IMDs.
- Section 4 investigates on the validity of the developed IM3 and IM5 model with a GaN MA DUT$_1$ dedicated to operate at microwave frequency f_{01}.
- Section 5 focuses on the experimental validation of IM3 and IMD3 induced by GaN MA DUT$_2$, which operates at mm-wave frequency f_{02}.
- Section 6 discusses the potential applications of the proposed IM model of MA NL, notably for the 5G and 6G communication system EMI effect minimization.
- Last, Section 7 is the paper's conclusion.

2. THEORY OF MICROWAVE AMPLIFIER INTERMODULATION MODELLING

This section presents the modelling theory of MA IM investigated in this work.

2.1. Methodology of Amplifier Modelling Methodology for Communication System Application

First and foremost, we have adopted the method of a developed modelling process, which can be organized in eight successive steps illustrated in the flowchart of Fig. 1.

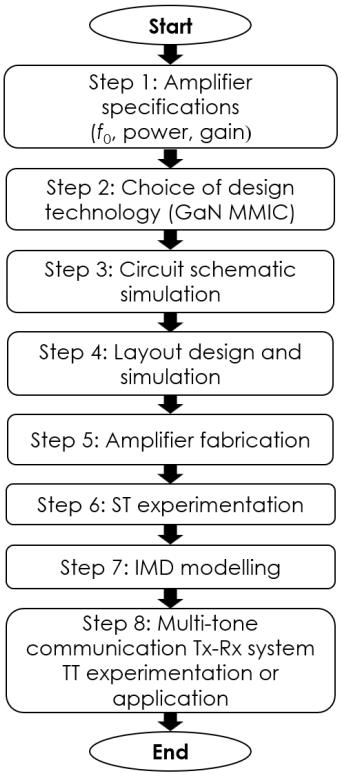

FIGURE 1. Flowchart illustrating the developed modelling process method and application.

The main contribution to the present modelling method concerns:

- The empirical coefficient extraction-obtaining $k_n = \{1, 3, 5, ...\}$ directly from measured ST harmonics;
- The predictive formulation-deriving explicit IM3/IM5 expressions for TT inputs before actual TT tests;
- The MA NL modelling application relevance directly addressing EMI in multi-carrier systems as demonstrated later in Subsection 6.3. This model will be useful for the development of a practical predictive tool.

To do this, the NL zones of the MA analysis are defined in the next subsection.

2.2. Definition on the Nonlinear (NL) Zones of Microwave Amplifier (MA) Single Tone (ST) Response

First of all, let us consider the ST synoptic diagram of MA depicted in Fig. 2 interacting with a harmonic input signal v_{in} having power P_{in} to generate an output v_{out} having power denoted by P_{out}. The developed NL modelling is based on the characterization of P_{out} versus P_{in} by using the ST harmonic input:

$$v_{in}(t) = A\cos(\omega_0 t) \tag{1}$$

specified by amplitude A and operating frequency $f_0 = \omega_0/(2\pi)$. The MA is supposed to operate in the linear, weakly NL (WNL) and strongly NL (SNL) regimes, which can be associated with the power levels denoted by Q_L, Q_{WNL}, and Q_{SNL}, respectively:

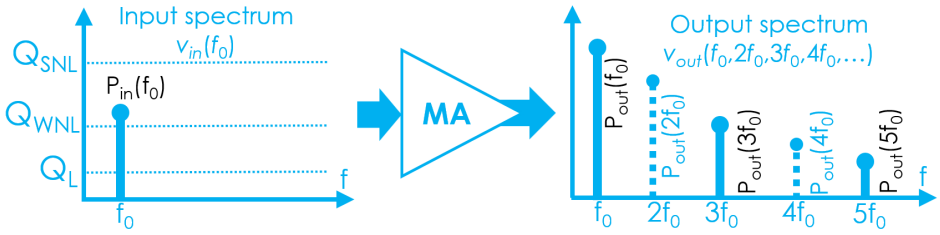

FIGURE 2. MA input and output spectra illustrating the ST method.

- (i) For $0 < A \leq Q_L$, the MA exhibits a linear behaviour with the gain:

$$g = \frac{P_{out}}{P_{in}}, \tag{2}$$

and the fundamental output voltage is denoted by:

$$v_{out}(t) = A_{out}\cos(\omega_0 t), \tag{3}$$

with the amplitude:

$$A_{out} = k_1 A. \tag{4}$$

- (ii) For $Q_L < A \leq Q_{WNL}$, the MA output voltage is expressed in a polynomial WNL model with consideration of harmonics.
- (iii) For $Q_{WNL} < A \leq Q_{SNL}$, the MA output voltage starts reaching the saturation level:

$$A_{out}(f_0) = V_{sat}. \tag{5}$$

Therefore, the output power can be assumed equal to:

$$P_{out}(f_0) = P_{sat}. \tag{6}$$

The amplitudes of ST MA NL response harmonics are defined in the next subsection.

2.3. Intermodulation Nonlinear Response of Microwave Amplifier under Single Tone Excitation

If the MA is memoryless, by taking real coefficients k_n with indices $n = 1, 2, 3, ...$, the corresponding output voltage can be expressed as the Volterra power series of the t-time dependent input signal:

$$v_{out}(t) = \sum_{n=0}^{\infty} k_n v_{in}^n(t). \tag{7}$$

As highlighted in Fig. 1, the n^{th}-order harmonic amplitude depends on the input one containing NL zone delimited by Q_1, Q_3, Q_5, ... By trigonometric linearization, this output signal with an ST input can be rewritten as:

$$v_{out}(t) = \sum_{n=0}^{\infty} A_{out}(nf_0)\cdot\cos(n\omega_0 t). \tag{8}$$

In the WNL operation zone, the output amplitude including n^{th} ($n \geq 3$) odd harmonic of the fundamental frequency f_0, which is derived from (7), is generally formulated as:

$$A_{out}(f_0) \approx k_1 A + \sum_{m=1}^{n} \frac{k_{2m+1}}{2^{2m}} \begin{pmatrix} 2m+1 \\ m \end{pmatrix} A^{2m+1}. \tag{9}$$

We calculated the amplitudes by considering harmonics up to $n = 7$. First, the output voltage amplitude at the fundamental frequency f_0 can be written as:

$$A_{out}(f_0) \approx A\left(k_1 + \frac{3k_3A^2}{4} + \frac{5k_5A^4}{8} + \frac{35k_7A^6}{64}\right). \tag{10}$$

The coefficients k_n for $n = \{1, 3, 5, 7\}$ can be determined from the measured output spectrum by using (10) and MATLAB fitting optimization. Then, the high-order harmonics at $3f_0$, $5f_0$, and $7f_0$ are expressed by, respectively:

$$A_{out}(3f_0) \approx \frac{A^3}{4}\left(k_3 + \frac{5k_5A^2}{4} + \frac{21k_7A^5}{16}\right), \tag{11}$$

$$A_{out}(5f_0) \approx \frac{A^5}{16}\left(k_5 + \frac{7k_7A^7}{16}\right), \tag{12}$$

$$A_{out}(7f_0) \approx \frac{k_7A^7}{64}. \tag{13}$$

The harmonic amplitude of MA NL response with TT excitation was derived from the ST ones. The obtained analytical responses are discussed in the next subsection.

2.4. Nonlinear Response of Microwave Amplifier under Two-Tone Excitation

The synoptic diagram of the NL test with TT input voltage v_{in} is illustrated in Fig. 3. The TT NL test consists in measuring IM_m with $m = \{3, 5\}$, which is generated by combined fundamental frequency components f_1 and f_2. By assuming $f_1 < f_2$ and:

$$\Delta f = f_2 - f_1 \ll f_0, \tag{14}$$

the two-tone components of v_{in} are expressed as:

$$v_{1,2}(t) = A\cos(\omega_{1,2}t), \tag{15}$$

with the amplitude A and angular frequency $\omega_{1,2} = 2\pi f_{1,2}$. To investigate the NL effect analytically, the TT input signal:

$$v_{in}(f_1, f_2) = v_1(f_1) + v_2(f_2), \tag{16}$$

can be expressed as:

$$v_{in}(t) = A\left[\cos(\omega_1 t) + \cos(\omega_2 t)\right]. \tag{17}$$

In this case, the fundamental output amplitude at f_0, which is established from (8) in function of NL coefficients k_m, is approximated as:

$$A_{out}(f_1) \approx \frac{A}{\sqrt{2}}\left(k_1 + \frac{9k_3A^2}{4} + \frac{25k_5A^4}{4} + \frac{1225k_7A^6}{64}\right). \tag{18}$$

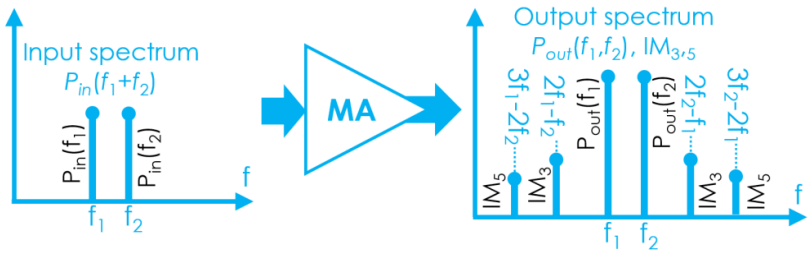

FIGURE 3. MA input and output spectra illustrating the TT method.

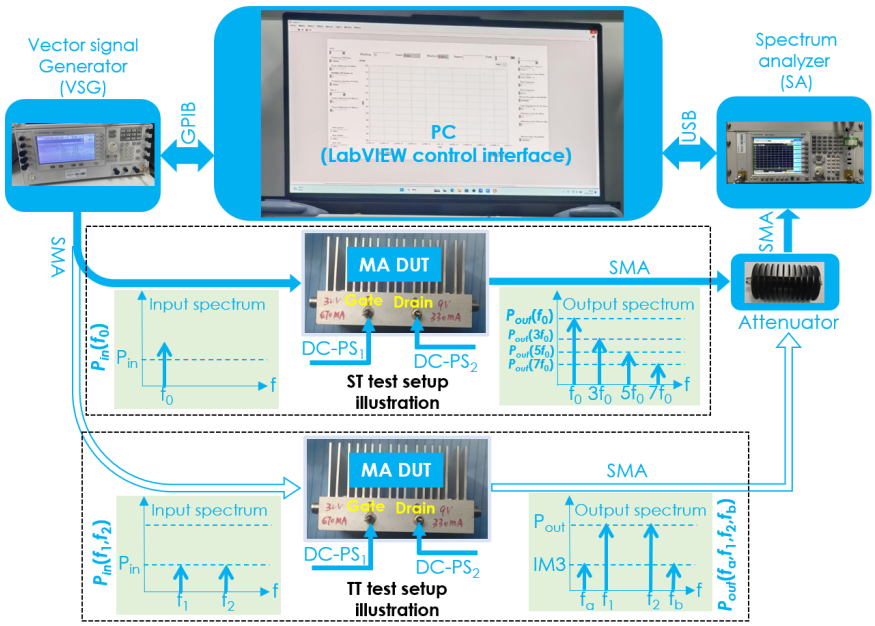

FIGURE 4. Synoptic diagram illustrating the ST and TT NL test setups of the GaN MA DUTs.

The IM_3 and IM_5 amplitudes at the harmonic frequencies $f_{IM3} = \{2f_1 - f_2, 2f_2 - f_1\}$ and $f_{IM5} = \{3f_1 - 2f_2, 3f_2 - 2f_1\}$ can be approximated as:

$$IM_3(2f_2 - f_1) \approx \frac{A^3}{4\sqrt{2}}\left(3k_3 + \frac{25k_5A^2}{2} + \frac{735k_7A^4}{16}\right), \quad (19)$$

$$IM_5(3f_2 - 2f_1) \approx \frac{A^5}{8\sqrt{2}}\left(5k_5 + \frac{245k_7A^2}{8}\right). \quad (20)$$

The experimental validation of the developed IM amplitude equations will be discussed in the following section.

3. DESCRIPTION OF AMPLIFIER IM3 AND IM5 EXPERIMENTAL SETUP

The present section is dedicated to the description of the experimental setup of the MA IM3 and IM5 measurements in the microwave and mm-wave frequencies. Then, the specifications of the test instruments are also discussed.

3.1. Description of the MA NL Characterization Experimental Setup

To perform the NL characterization of the considered DUT GaN MAs, both IM3 and IM5 were measured. Doing this, an automatic test setup enabling to sweep automatically both amplitude A and harmonic input signal operating with frequency f_0 of input signals was developed as illustrated by the synoptic diagram displayed in Fig. 4. The measurement results from the ST and TT test around f_0 enable obtaining the expected GaN MA NL characteristics.

Both the ST and TT tests were carried out with the automatic LabVIEW-based test bench developed in [7, 8] by using Agilent E8267D vector signal generator (VSG) and Agilent E4447A spectrum analyzer (SA) as illustrated in Fig. 3. It is worth noting that the attenuation and loss can be assessed from the output signal of the DUTs.

The employed instruments for NL characterization of the GaN MAs are specified in the next subsection.

3.2. Specifications of the Employed Instruments during the NL Test

The performances of the instruments play a key role in performing a relevant test of the MA IM3 and IM5. One emphasizes that each instrument has $R_0 = 50\,\Omega$ port characteristic impedance. Table 1 indicates the technical specifications of each instrument employed during the MA NL test measurement.

TABLE 1. Specifications of employed instruments for the ST and TT NL tests of GaN MAs.

Designation	References	Specification
PC	ThinkPad	Equipped with Windows 10 OS and LabVIEW 20
VSG	Agilent E8267D	250 kHz–44 GHz
SA	Agilent E4447A	3 Hz–42.98 GHz
DC PS	Agilent E3648A	PS_1 (0–8 V, 5 A/0-20 V, 2.5 A)
	Agilent E3632A	PS_2 (0–15 V, 5 A/0–30 V, 4 A)
Attenuator	2.92TS20-20-40	20 dB

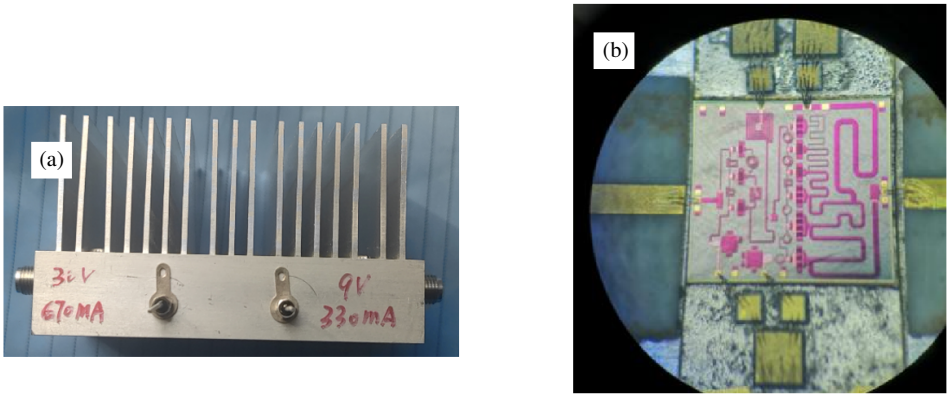

FIGURE 5. Photos of (a) packaging and (b) MMIC GaN MA DUT_1 dedicated to operate @ $f_{01} = 2.4$ GHz.

During the experimental tests, the considered GaN MA DUTs were fed by the Agilent E3632A as the gate power supply (PS_1) and the Agilent E3648A as the drain power supply (PS_2).

3.3. Justification of the NL DUTs Choice

The choice of the two DUTs investigated in the present research work was strategic to demonstrate the robustness and general applicability of the developed modeling method. The main frequency specifications of the tested MAs are:

- DUT_1 ($f_{01} = 2.4$ GHz): This DUT represents a common microwave frequency with a relatively narrowband design. It serves as a baseline validation under typical conditions.
- DUT_2 ($f_{02} = 24$ GHz/6–30 GHz band): This DUT represents a millimetre-wave frequency with a wideband design. It presents a more challenging environment with potential for greater dispersion.

By successfully applying our model to amplifiers with different center frequencies and different bandwidth characteristics, we provide strong evidence that the methodology is not limited to a specific device type but is a general technique for GaN amplifier NL characterization across relevant RF and millimeter-wave bands.

The obtained test results are explored in the following subsections.

4. IM3 AND IM5 MODEL VALIDATION WITH GALLIUM NITRIDE AMPLIFIER DUT_1

The results confirming the relevance of the IM3 and IM5 models with GaN MA DUT_1 prototype are investigated in this section.

4.1. Single Tone (ST) Test and Characterization Results of Gallium Nitride (GaN) Microwave Amplifier under Study

The photos of packaging and MMIC GaN MA DUT_1 expected to be characterized at $f_{01} = 2.4$ GHz are presented in Fig. 5(a) and Fig. 5(b), respectively. The technological characteristics of considered DUT_1 are indicated in Table 2. This DUT was designed to operate under a nominal gain $g(f_{01}) = 38$ dB in the frequency band 2–6 GHz.

TABLE 2. Characteristics of DUT_1.

Description	Characteristics
Technology	250-nm MMIC
Reference	INPA-0108-P40A
Drive PA	IPA-0206B
Substrate	Rogers 4350B
Electrical interconnect	Gold Wire Bonding

To carry out the DUT_1 ST test, the VSG was adjusted from the LabVIEW front panel to automatically vary P_{in} from -35 to 0 dBm.

The following subsection discusses the test results illustrating the P_{out} vs P_{in} power transfer characterization.

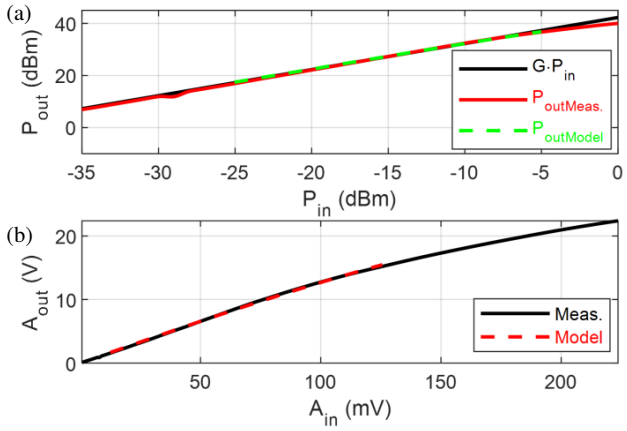

FIGURE 6. Ideal, measured, and modelled (a) power (P_{out}-P_{in}), and (b) voltage amplitude (A_{out}-A_{in}) characteristics of the GaN MA DUT$_1$.

4.2. P_{in}-P_{out} Power Characterization of the Tested MA

The WNL behavior (WNLB) is illustrated by the P_{out}-P_{in} transfer characteristic power and A_{out}-A_{in} amplitude characteristics displayed in Fig. 5(a). Knowing from (2), the output power of linear MA can be ideally determined by:

$$P_{out,ideal} = g \times P_{in}. \tag{21}$$

Emphatically, the "Ideal", measured ("Meas."), and modelled characteristics are plotted in black solid, red solid, and green dashed curves in Fig. 6(a), respectively.

Assuming that the SA and DUT$_1$ are well matched, the input and output voltage magnitudes at test frequency f_0 can be calculated from the relationship:

$$\begin{cases} A_{in}(f_0) = \sqrt{10^{\frac{P_{in,\,\mathrm{dBm}}(f_0)+30}{10}} R_0} \\ A_{out}(f_0) = \sqrt{10^{\frac{P_{out,\,\mathrm{dBm}}(f_0)+30}{10}} R_0} \end{cases}. \tag{22}$$

The output amplitudes of voltage modeled with the Volterra series expressed in (1) fit very well with the measured ones plotted in Fig. 6(b).

The comparison of modelled and experimental results of IM3/IMD3 and IM5/IMD5 from the DUT$_1$ is examined in the following subsection.

4.3. Comparison between Modeled and Measured IM3 AND IM5 Results of DUT$_1$

In this case, IM3 and IM5 were modelled in the WNL zone delimited by $P(Q_L) = -25$ dBm and $P(Q_{WNL}) = -5$ dBm. The MA NL coefficients were extracted by the MATLAB least mean square optimization procedure for A_{out} according to Equation (4). Table 3 shows the extracted MA NL coefficients k_i approximated up to the 7th-order harmonic.

TABLE 3. NL model coefficients of MA DUT$_1$.

Coefficients	k_1	k_3	k_5	k_7
Value	147	−751	−141	−25

By taking $f_1 = 2.399$ GHz and $f_2 = 2.401$ GHz, the DUT$_1$ TT test with the automatic test bench described in [7, 8] was performed by varying simultaneously the input amplitudes $A_1 = A_2 = A$ from −35 to 0 dBm.

With the extracted coefficients k_i, the values of IM3($2f_1 - f_2 = 2.397$ GHz) = IM3($2f_2 - f_1 = 2.403$ GHz) and IM5($3f_1 - 2f_2 = 2.395$ GHz) = IM5($3f_2 - 2f_1 = 2.405$ GHz) were calculated for $P(Q_L) < P_{in} \leq P(Q_{WNL})$ by using (11) and (12). The obtained characteristics of the IM3 and IM5 (solid curves) are in a very good agreement with measured ones (dashed curves) by fixing the SA noise floor to −65 dBm (Fig. 7(a)). It is worth denote that in the considered WNL range, the IM3 and IM5 characteristics increase proportionally to $3P_{in}$ or $5P_{in}$ slope when P_{in} increases. The difference between the modelled and measured values of $\max(|\mathrm{IM3_{model}} - \mathrm{IM3_{meas}}|) < 3$ dB and $\max(|\mathrm{IM5_{model}} - \mathrm{IM5_{meas}}|) < 5$ dB is assessed. The discrepancies between the computed model and experimentation can be explained by the GaN MA memory effect and measurement system errors. Furthermore, the calculated characteristics $\mathrm{IMD3_{dB}} = P_{out,\mathrm{dB}} - \mathrm{IM3_{dB}}$ and $\mathrm{IMD5_{dB}} = P_{out,\mathrm{dB}} - \mathrm{IM5_{dB}}$ of the DUT$_1$ are displayed in Fig. 7(b) in comparison with those measured. Typical IMD variation, which decreases when P_{in} increases, is observed in the WNL range.

The NL characterization of another MA represented by DUT$_2$ is explored in the next section.

5. IM3 AND IMD3 MODEL VALIDATION WITH GALLIUM NITRIDE AMPLIFIER DUT$_2$ @ $f_{02} = 24$ GHz

This section discusses the validation of the developed IM model in millimeter higher frequencies with another GaN MA DUT$_2$.

5.1. MA DUT$_2$ Prototype

The photos of the fabricated and tested GaN MA DUT$_2$ prototype are shown in Fig. 8. It is dedicated to operate around $f_{02} = 24$ GHz.

The characteristics of tested DUT$_2$ are addressed in Table 4.

TABLE 4. Characteristics of DUT$_2$.

Description	Characteristics
Technology	MMIC 150 nm
Reference	NC116139C-2128P10
Substrate	RO4350C
Electrical interconnect	Gold Wire Bonding
Output	WR28 waveguide

The MA is intended to operate with gain $g(f_{02}) = 44$ dB in the frequency range 6 GHz–30 GHz. The ST test results are discussed in the next subsection.

5.2. ST Characterization Test Results of MA DUT$_2$

In the case, DUT$_2$ operates at $f_{02} = 24$ GHz with ideal gain $g(f_{02}) = 27.7$ dB. The obtained ST test results are plotted in Fig. 9. One can emphasize that the ST was performed by gradually increasing P_{in} from $P_{in,\min} = -20$ dBm to $P_{in,\max} = 10$ dBm with 1 dBm step. Fig. 9(a) and Fig. 9(b) show the ideal,

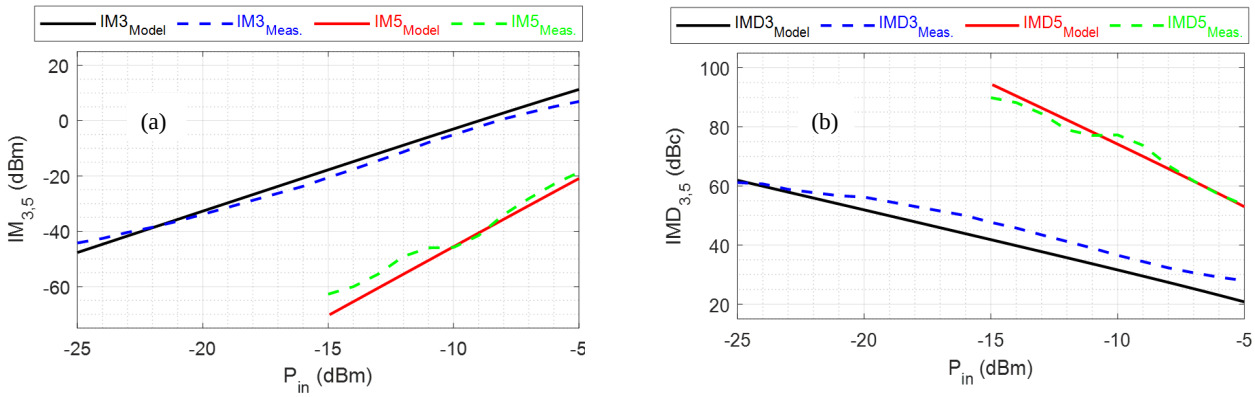

FIGURE 7. Modelled and measured (a) intermodulation product power (IM_3, IM_5) in dBm and (b) relative intermodulation distortion (IMD_3, IMD_5) in dBc of DUT_1.

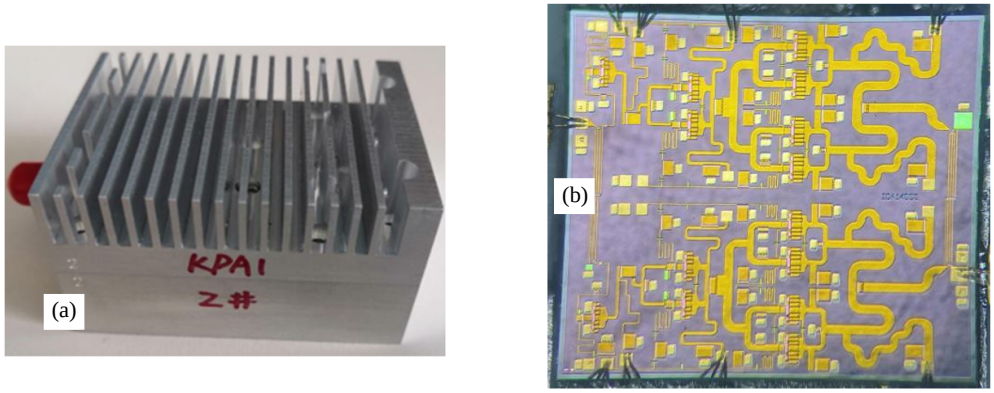

FIGURE 8. Photos of (a) packaging and (b) MMIC GaN MA DUT_2 dedicated to operate @ $f_{02} = 24$ GHz.

measured, and modelled P_{out}-P_{in} power and voltage amplitude characteristics.

The diagram illustrates the WNLB in the P_{in} range delimited between $P(Q_L) = -20$ dBm and $P(Q_{WNL}) = -3$ dBm. Again, the DUT_2 NL coefficients were extracted by the MATLAB optimization procedure in the WNL regime. The obtained coefficients limited to the 7th-order harmonic are given in Table 5.

TABLE 5. NL model coefficients of MA DUT_2.

Coefficients	k_1	k_3	k_5	k_7
Value	149	−1221	4345	−4979

Figure 9(a) compares the P_{out}-P_{in} power ST characteristic, illustrating that the calculated output power plotted in red dashed curve is in very good agreement with experimental results plotted in cyan solid curve.

The obtained GaN MA IM3 and IMD3 validation results are discussed in the next subsection.

5.3. Comparison between Modeled and Measured Results of DUT_2

During the TT input signals of DUT_2, the amplitudes of $P_{in}(f_1)$ and $P_{in}(f_2)$ were automatically and gradually increased from $P_{in,\min} = -20$ dBm to $P_{in,\max} = 10$ dBm with 1 dBm step. The TT output spectrum within the frequency band [23.95 GHz, 24.05 GHz] is displayed in Fig. 10.

The extracted IM3 and IMD3 were displayed in Fig. 11(a) and Fig. 11(b), respectively. Consequently, the measured (cyan solid curve) and modelled (red dashed curve) characteristics of IM3($2f_1 - f_2 = 23.985$ GHz) = IM3($2f_2 - f_1 = 24.015$ GHz), which are defined by (9), are plotted in Fig. 11(a) for the input fundamentals fixed to $f_1 = 23.995$ GHz and $f_2 = 24.005$ GHz with the same amplitudes $A_1 = A_2 = A$. In this case, we obtain $\max(|\text{IM3}_{\text{model}} - \text{IM3}_{\text{meas}}|) < 5$ dB. The IM3 increases by about 20 dB when P_{in} increases to 5 dB. The DUT_2 IMD3 was calculated as IMD3 = P_{out} − IM3 by adjusting the VSG modulation mode to have the TT signal. The results highlight that the IMD3 varies from about 17 dB to 55 dB for DUT_2 (Fig. 11(b)).

The potential applications of the developed IM model are discussed in the next section.

6. ANALYSES AND POTENTIAL APPLICATIONS OF THE DEVELOPED IM3 AND IM5 MODELS OF MICROWAVE AMPLIFIER NONLINEARITY

After brief comments on the GaN MA NL characteristics, the potential applications of the developed IM modelling are itemized in this section.

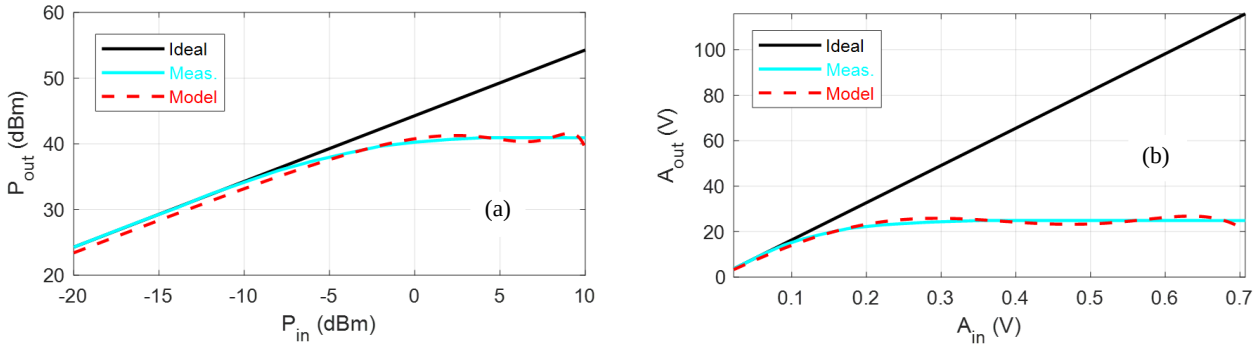

FIGURE 9. Comparison of ideal, measured, and modelled (a) P_{out}-P_{in} power transfer and (b) voltage amplitude characteristic of GaN MA DUT$_2$.

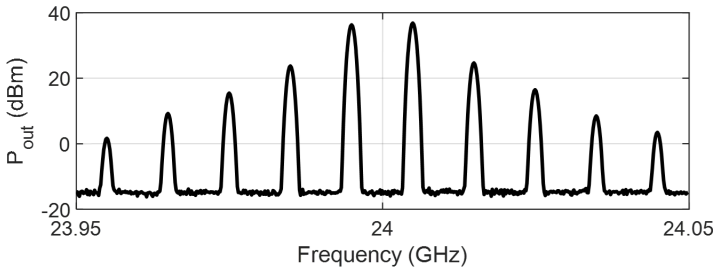

FIGURE 10. MA output spectrum with $P_{in} = 15$ dBm.

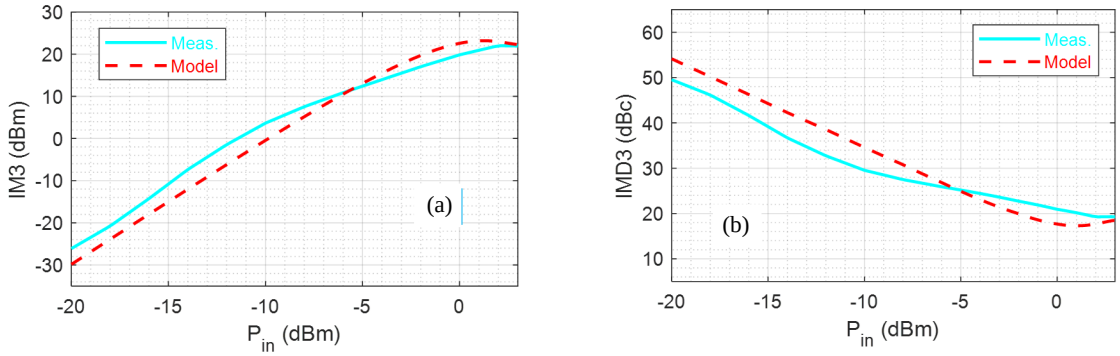

FIGURE 11. Measured and modelled (a) IM3 and (b) IMD3 characteristics of DUT$_2$.

6.1. Remark and Comment on the Modelled Microwave Amplifier Intermodulation Distortion

Further interpretation and analyses of the previous measurement results and the proposed IM models are commented on in this subsection. The following remark can be emphasized from the obtained modeled and experimental results of the understudied MAs:

- The modelled IMD3 characteristics are in good agreement with theory, but in practice, they can only be close to measurement due to factors such as signal source and attenuation;
- From the calculated and measured IM3 characteristics plotted in Fig. 8(a) and Fig. 11(a), one finds that there are some discrepancies between them, which can be attributed to the experimental inaccuracies;
- As P_{in} increases gradually, the DUT$_1$ MA enters the WNL region. Based on the behavioural plot of Fig. 8(b), the IM3 and IM5 characteristics' increase rate is greater than the fundamental component one;
- Moreover, as P_{in} increases gradually, the IMD3 gradually decreases when $P_{out} \approx 40.5$ dBm. Therefore, the IMD3 of MA are greater than 50 dBc if $P_{in} < -20$ dBm;
- The measured values of the DUT IMD3 and IMD5 characteristics meet the industrial design requirements and correspond to weak NL distortion.

6.2. Comparative Study of the Present Work and Existing Ones

The developed method of NL active device modelling and characterization presents certain advantages, notably to facilitate the design process and minimization of EMI in the Tx-Rx communication system. Compared to the existing ones in the literature [7, 8], the main advantages are the fact that the proposed modelling methodology enables taking into account the IM modelling and experimental analyses. The notable advan-

tages of the study are the ability of the developed model to help microwave and millimeter wave design engineers in the future. The carried-out study permits the prediction of the performance of 5G and 6G Tx-Rx communication system in function of the NL device.

6.3. Discussion on Potential Applications of the Developed Microwave Amplifier Intermodulation Model

To avoid the communication quality degradation of RF, microwave, and mm-wave communication systems, the developed NL IM model of GaN MA can constitute a particularly interesting solution. The following items explain the usefulness of the developed model for MA and communication system designers and manufacturers:

- During the design of microwave active circuits, the NL model can be used to minimize the unintentional effect on the communication performance.
- It helps as well to choose the adequate active components, such as MA constituting the Tx-Rx or front-end chain.
- To reduce the unintentional EMI risk in the multichannel Tx-Rx communication system.
- Then, such a developed model of DUT IMD3 and IMD5 meets industrial design requirements and corresponds to weak NL distortion.

7. CONCLUSION

Based on the fundamental mathematical theory of limited expansion and by considering a positive integer $m = 1, 2, 3, ...$, an efficient NL modelling of m^{th}-order IM associated with MA was presented. The developed models were analytically developed based on the Volterra series expression of the output voltage versus the input one. The Volterra series coefficients were empirically determined from the ST test of MA prototyping. Then, the IM(m) powers and their interference with the fundamental frequencies of the TT test were formulated.

The IM(m) NL model validity was verified with GaN MA DUTs at two different frequencies 2.4 GHz and 24 GHz. The obtained results confirm the possibility to analyze the IM(m) with the TT experimental in the weak NL zone.

The extension of the developed model by taking into account the GaN MA memory effect [18, 19] and also with the three- or multi-tone tests is currently in progress.

ACKNOWLEDGEMENT

The developed research work is supported by in part by Natural National Science Foundation of China (NSFC) research program via Grant No. 62350610268 and Grant No. 62371241 and in part by Beijing Natural Science Foundation under Grant No. L233002.

REFERENCES

[1] Saad, W., M. Bennis, and M. Chen, "A vision of 6G wireless systems: Applications, trends, technologies, and open research problems," *IEEE Network*, Vol. 34, No. 3, 134–142, May/Jun. 2020.

[2] Bayram, Y., J. L. Volakis, S. K. Myoung, S. J. Doo, and P. Roblin, "High-power EMI on RF amplifier and digital modulation schemes," *IEEE Transactions on Electromagnetic Compatibility*, Vol. 50, No. 4, 849–860, Nov. 2008.

[3] Fiori, F. L. and P. S. Crovetti, "Prediction of high-power EMI effects in CMOS operational amplifiers," *IEEE Transactions on Electromagnetic Compatibility*, Vol. 48, No. 1, 153–160, Feb. 2006.

[4] Abuelma'atti, M. T., "Analysis of the effect of radio frequency interference on the DC performance of bipolar operational amplifiers," *IEEE Transactions on Electromagnetic Compatibility*, Vol. 45, No. 2, 453–458, May 2003.

[5] Mordachev, V. I., "Automated double-frequency testing technique for mapping receive interference responses," *IEEE Transactions on Electromagnetic Compatibility*, Vol. 42, No. 2, 213–225, May 2000.

[6] Panigrahi, S. R. and D. Rönnow, "Evaluating nonlinear distortion of single and dual channel excitation of an amplifier at 24 GHz," *Microwave and Optical Technology Letters*, Vol. 63, No. 9, 2315–2319, 2021.

[7] Cheng, X., F. Wan, V. Mordachev, E. Sinkevich, X. Chen, and B. Ravelo, "Nonlinear microwave device LabVIEW automatic test bench: Double-frequency IMD3 characterization," *Progress In Electromagnetics Research B*, Vol. 108, 47–59, 2024.

[8] Du, H., F. Wan, V. Mordachev, E. Sinkevich, X. Chen, and B. Ravelo, "EMI characterization from GaN power amplifier nonlinearity test for 16-QAM 5G communication," *Radioengineering*, Vol. 33, No. 4, 669–680, 2024.

[9] Fu, K., C. L. Law, and T. T. Thein, "Test bed for power amplifier behavioral characterization and modeling," *Measurement*, Vol. 46, No. 8, 2735–2745, 2013.

[10] Palumbo, G. and S. Pennisi, "High-frequency harmonic distortion in feedback amplifiers: Analysis and applications," *IEEE Transactions on Circuits and Systems I: Fundamental Theory and Applications*, Vol. 50, No. 3, 328–340, Mar. 2003.

[11] Miao, Y. and Y. Zhang, "Distortion modeling of feedback two-stage amplifier compensated with Miller capacitor and nulling resistor," *IEEE Transactions on Circuits and Systems I: Regular Papers*, Vol. 59, No. 1, 93–105, 2012.

[12] Minasian, R. A., "Intermodulation distortion analysis of MESFET amplifiers using the Volterra series representation," *IEEE Transactions on Microwave Theory and Techniques*, Vol. 28, No. 1, 1–8, Jan. 1980.

[13] Lima, E. G., T. R. Cunha, H. M. Teixeira, M. Pirola, and J. C. Pedro, "Base-band derived volterra series for power amplifier modeling," in *2009 IEEE MTT-S International Microwave Symposium Digest*, 1361–1364, Boston, MA, USA, 2009.

[14] Celik, A., Z. Zhang, and P. P. Sotiriadis, "A state-space approach to intermodulation distortion estimation in fully balanced bandpass Gm-C filters with weak nonlinearities," *IEEE Transactions on Circuits and Systems I: Regular Papers*, Vol. 54, No. 4, 829–844, Apr. 2007.

[15] Shi, G., "Symbolic distortion analysis of multistage amplifiers," *IEEE Transactions on Circuits and Systems I: Regular Papers*, Vol. 66, No. 1, 369–382, 2019.

[16] Maffezzoni, P., "Efficient multiparameter sensitivity computation of amplifier harmonic distortion," *IEEE Transactions on Circuits and Systems II: Express Briefs*, Vol. 54, No. 3, 257–261, 2007.

[17] Fiori, F., "A new nonlinear model of EMI-induced distortion phenomena in feedback CMOS operational amplifiers," *IEEE Transactions on Electromagnetic Compatibility*, Vol. 44, No. 4, 495–502, Nov. 2002.

[18] Bosch, W. and G. Gatti, "Measurement and simulation of memory effects in predistortion linearizers," *IEEE Transactions on Microwave Theory and Techniques*, Vol. 37, No. 12, 1885–1890, Dec. 1989.

[19] Yang, G., H. Li, W. Qiao, C. Jiang, Q. Liu, G. Wang, and F. Liu, "Digital predistortion based on sample selection with memory effect," *International Journal of RF and Microwave Computer-Aided Engineering*, Vol. 32, No. 2, e22976, 2022.